A&A 637, A83 (2020)
https://doi.org/10.1051/0004-6361/202037695

Astronomy & Astrophysics

Subsequent outbursts of the same EXor source possibly present similar features

T. Giannini[1], A. Giunta[2], D. Lorenzetti[1], G. Altavilla[1,2], S. Antoniucci[1], F. Strafella[3], and V. Testa[1]

[1] INAF-Osservatorio Astronomico di Roma, Via Frascati 33, 00078 Monte Porzio Catone, Italy
e-mail: teresa.giannini@inaf.it
[2] ASI – Agenzia Spaziale Italiana, Via del Politecnico, 00133 Roma, Italy
[3] Dipartimento di Matematica e Fisica, Universitá del Salento, 73100 Lecce, Italy

Received 10 February 2020 / Accepted 28 March 2020

ABSTRACT

Context. V1118 Ori is a classical EXor source whose light curve has been monitored, although not continuously, over the past 30 years. This source underwent a powerful outburst in 2005, followed by 10 years of quiescence and a less intense outburst in 2015. In 2019, a new intense brightness increase was observed ($\Delta g \sim 3$ mag).
Aims. This new accretion episode offers the opportunity to compare the photometric and spectroscopic properties of multiple outbursts of the same source. This allows us to highlight the differences and similarities among various events by removing any possible bias related to the intrinsic properties of the star-disk system.
Methods. We discovered the 2019 V1118 Ori outburst by examining the g-band light curve acquired by the Zwicky Transient Facility and followed the declining phase with the Rapid Eye Mount telescope in the $griz$ bands. Two near-infrared spectra were also acquired at different brightness stages with the Large Binocular Telescope.
Results. The last event shows the following characteristics: (1) an amplitude similar to that of 2015 and lower than that of 2005; (2) a duration of less than one year as in previous events; (3) a increasing (decreasing) speed of 0.018 (0.031) mag day^{-1}, which is different from previous cases; (4) a gradually blueing of the $[g-r]$ color is observed over time, while the $[r-i]$ color remains roughly unchanged; (5) with few exceptions, the near-infrared lines (mainly H I recombination) are the same as those observed in 2015; and (6) the mass accretion rate peaks at $\dot{M}_{\rm acc} \sim 10^{-7}\,M_{\odot}$ yr^{-1} and decreases in about a month down to a few $10^{-8}\,M_{\odot}$ yr^{-1}.
Conclusions. Our analysis shows that the comparison of data from different outbursts of the same source is a nontrivial exercise, which allows us to obtain important clues that are useful to drive theoretical efforts toward a better understanding of the EXor phenomenon.

Key words. stars: pre-main sequence – stars: individual: V1118 Ori – stars: variables: T Tauri, Herbig Ae/Be

1. Introduction

Eruptive variables belong to a class of pre-main-sequence objects usually divided into two subclasses: EXor (Herbig 1989) and the more energetic FUor (Hartmann & Kenyon 1985) systems, which both present an intermittent variability related to an unsteady mass accretion rate. The membership to either subclass depends on the different properties, such as the amplitude and duration of the bursts, the recurrence time between subsequent bursts, and the mass accretion rate. A comprehensive account of the properties of both EXors and FUors is given by Audard et al. (2014).

In general terms, the observed features that define the EXor-class membership are the occurrence on timescales of years of short-term outbursts (typically lasting several months) with amplitude ΔV of about 3–5 mag at optical and near-infrared (near-IR) wavelengths and spectra characterized by strong H I recombination lines and other atomic permitted lines (e.g., Herbig 2008; Lorenzetti et al. 2009; Sicilia-Aguilar et al. 2012; Kóspál et al. 2011).

Although EXor outbursts are known to be associated with magnetospheric accretion events from the circumstellar disk (Shu et al. 1994), their nature is still very uncertain and no specific models have been developed so far. Therefore, the theoretical framework developed by Hartmann & Kenyon (1985) for FU Orionis objects is also widely adopted for EXors. More specific efforts have been performed in the last decade (D'Angelo & Spruit 2010; Vorobyov & Basu 2015), however difficulties arise in predicting the relatively short cycle time of the episodic accretion phenomena and there are only suggestions about the mechanism responsible for the outburst onset. These include thermal instabilities (e.g., Bell & Lin 1994), the presence of a massive planet (Lodato & Clarke 2004), and close interactions in a binary system (Bonnell & Bastien 1992).

Observational inputs to the current theoretical framework can be obtained by comparing the results of both photometric and spectroscopic observations at optical and near-IR frequencies of successive outbursts of the same source. This comparison allows us to highlight similarities and differences of multiple events in the same star-disk system and to remove all possible biases often introduced when considering outbursts of sources with different masses, luminosities, or evolutionary stages. In this way, the uncontaminated interplay between the outburst parameters (amplitude, duration of both rising and declining phases, and fluctuations of the local extinction) can be more accurately determined.

A suitable target for this kind of investigation is the classical EXor V1118 Ori, a source that has been monitored over the past 30 years by several authors (Audard et al. 2005, 2010 and references therein). We have been following V1118 Ori

for more than 10 years observing both quiescent and outbursting periods (Lorenzetti et al. 2006, 2007, 2015). In particular, our monitoring of the outburst occurred in the period 2015–2016 allowed us to estimate the evolution of the mass accretion rate (compared to the immediately precedent quiescence) from $0.3–20\times10^{-8}$ to $0.2–2\times10^{-6}\,M_{\odot}\,\mathrm{yr}^{-1}$ (Giannini et al. 2016, 2017). During 2017–2018 V1118 Ori went through a period of quiescence. In May 2019 we announced a new outburst (Giunta et al. 2019a), remarking on its peculiarity in terms of increasing and decreasing speeds (Giunta et al. 2019b). Our observations of this last event are presented in Sect. 2, while the results are discussed and compared with those of the previous outbursts in Sect. 3. Our final remarks are given in Sect. 4.

2. Observations and data reduction

2.1. Optical photometry

In the period 2018–2019 V1118 Ori was monitored in the g band with the Zwicky Transient Facility (ZTF)[1], which reported an increase of about two magnitudes (from $g\sim17$ to 15) between February and April 2019 (see Table 1). Owing to seasonal observability, subsequent observations could only start in late August when the source was still bright ($g\sim14.4$), but already in the declining phase. The quiescence was reached again in late November.

To increase the temporal coverage, we observed V1118 Ori with the ROSS2 optical camera installed on the 60 cm robotic telescope Rapid Eye Mount (REM) at La Silla (Chile). The observations were conducted in the g, r, z, i bands and covered mainly the declining phase from August to September 2019.

The images were reduced by using standard procedures for bad pixel removal, flat fielding, and bias and dark subtraction. The aperture photometry was then obtained using as calibrators several stars in the V1118 Ori field, whose optical magnitudes have been retrieved by the PAN-STARSS Data Release 2 (DR2) Photometric Catalog[2]. The photometric data are listed in Table 2.

Figure 1 depicts the g-band light curve. We certainly missed the outburst peak, which occurred in the period June–August 2019. Unfortunately, no *Gaia* passages on V1118 Ori were performed during this period because the closest in time were carried out on August 13 (Lattanzi, priv. comm.). No alert was issued at that time. The ROSS2 observations have partially filled the observational gap, allowing us to get the highest photometric point of both the rising and declining phases: on 9 May 2019 $g=14.56$ and on 12 August 2019 $g=14.00$.

To get a rough estimate of the peak brightness we fit with a straight line both the rising and declining light curves, which intersect at $g\sim13.8$ mag (see Sect. 3.1.1). This value is comparable to the peak reached in the 2015–2016 outburst (Giannini et al. 2016), as also shown in the historical light curve presented in Fig. 2.

2.2. Spectroscopy

Near-IR spectra were collected on October 1 (MJD 58757) and October 20, 2019 (MJD 58776). Both spectra were obtained with the 8.4 m Large Binocular Telescope (LBT) located in Mount Graham (Arizona, USA) using the LUCI2 spectrometer. The observations were conducted with the G200 grating (zJ and HK filters) covering the spectral ranges 0.9–1.20 μm and

[1] https://www.ztf.caltech.edu
[2] https://catalogs.mast.stsci.edu/panstarrs/

Table 1. Zwicky Transient Facility photometry.

MJD	Date	g (mag)
58204	27 Mar. 2018	17.15
58362	01 Sep. 2018	17.58
58365	04 Sep. 2018	17.54
58368	07 Sep. 2018	17.34
58371	10 Sep. 2018	17.24
58374	13 Sep. 2018	17.45
58377	16 Sep. 2018	17.48
58397	06 Oct. 2018	17.23
58425	03 Nov. 2018	17.50
58427	05 Nov. 2018	17.12
58428	06 Nov. 2018	17.15
58430	08 Nov. 2018	16.86
58431	09 Nov. 2018	17.19
58434	12 Nov. 2018	17.15
58437	15 Nov. 2018	16.70
58438	16 Nov. 2018	17.05
58439	17 Nov. 2018	16.96
58440	18 Nov. 2018	17.17
58443	21 Nov. 2018	17.19
58450	28 Nov. 2018	17.48
58462	10 Dec. 2018	17.24
58466	14 Dec. 2018	17.51
58469	17 Dec. 2018	17.74
58472	20 Dec. 2018	17.66
58476	24 Dec. 2018	17.44
58487	04 Jan. 2019	16.91
58509	26 Jan. 2019	16.82
58523	09 Feb. 2019	16.22
58542	28 Feb. 2019	16.64
58547	05 Mar. 2019	15.91
58557	15 Mar. 2019	16.06
58560	18 Mar. 2019	16.07
58573	31 Mar. 2019	16.00
58582	09 Apr. 2019	15.18
58717	22 Aug. 2019	14.41
58723	28 Aug. 2019	14.79
58726	31 Aug. 2019	14.40
58734	08 Sep. 2019	15.19
58737	11 Sep. 2019	14.81
58740	14 Sep. 2019	15.37
58745	19 Sep. 2019	15.52
58748	24 Sep. 2019	15.59
58750	26 Sep. 2019	15.58
58756	02 Oct. 2019	15.92
58763	09 Oct. 2019	15.64
58766	12 Oct. 2019	15.93
58767	13 Oct. 2019	16.07
58768	14 Oct. 2019	16.11
58775	19 Oct. 2019	16.38
58779	23 Oct. 2019	16.54
58780	24 Oct. 2019	16.60
58788	01 Nov. 2019	17.04
58799	12 Nov. 2019	16.85
58805	18 Nov. 2019	16.84
58812	25 Nov. 2019	17.41

Notes. Typical photometric errors are 0.05 mag.

Table 2. Rapid Eye Mount photometry.

MJD	Date	g (mag)	r (mag)	i (mag)	z (mag)
58612	09 May 2019	14.56	13.83	13.31	12.76
58707	12 Aug. 2019	14.00	13.59	12.99	12.60
58710	15 Aug. 2019	14.56	13.81	13.45	12.87
58713	18 Aug. 2019	14.49	13.74	13.34	12.74
58716	21 Aug. 2019	14.19	13.57	13.05	12.64
58719	24 Aug. 2019	14.77	13.99	13.48	12.96
58722	27 Aug. 2019	14.77	14.01	13.47	12.97
58727	01 Sep. 2019	14.56	13.73	13.32	12.83
58730	04 Sep. 2019	14.60	13.85	13.42	12.91
58733	07 Sep. 2019	15.00	14.32	13.86	13.20
58736	10 Sep. 2019	14.71	14.02	13.48	13.01
58739	13 Sep. 2019	15.52	14.62	14.24	13.52
58744	18 Sep. 2019	15.60	14.79	14.27	13.52
58747	21 Sep. 2019	15.59	14.74	14.41	13.72
58750	24 Sep. 2019	15.49	14.82	14.33	13.71
58753	27 Sep. 2019	15.69	14.99	14.49	13.85
58756	30 Sep. 2019	15.75	15.06	14.62	13.88

Notes. Typical photometric errors are 0.05 mag.

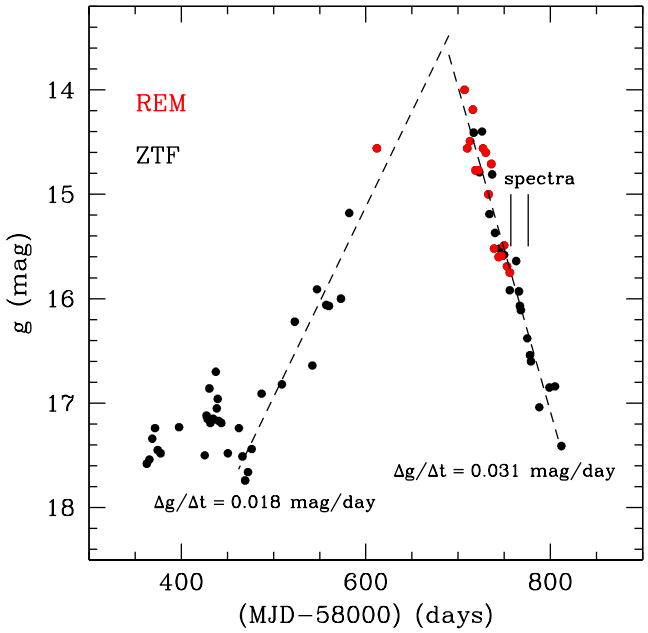

Fig. 1. Zwicky Transient Facility (black) and REM (red) g-band photometric points of the 2019 outburst of V1118 Ori. The two dashed lines indicate the linear fits to the points of the rising and declining phases, with indicated the values of their slopes (mag day^{-1}). Both have an uncertainty of 0.002 mag day^{-1}. Two continuous segments indicate the dates of the spectroscopic observations.

1.50–2.40 μm. We used the 0.″75 slit, corresponding to a spectral resolution between 1200 and 1700. The standard ABB′A′ technique was adopted to perform the observations, for a total integration time of 16 min for each spectrum.

Data reduction was carried out at the Italian LBT Spectroscopic Reduction Center[3], using scripts optimized for LBT observations. The spectral images were flat-fielded, sky-subtracted, and corrected for optical distortion in both spatial and spectral directions. The telluric features were removed by dividing the extracted spectra by that of a telluric standard star (observed on the same nights as the targets), once corrected for its intrinsic hydrogen absorption features. Wavelength calibration was obtained from arc lamps. The K-band acquisition image was used to estimate the photometry of V1118 Ori on the dates of the spectral observations ($K = 10.08$ on October 1 and $K = 10.70$ on October 20), which in turn was used for flux calibration of the HK spectral segments. The zJ spectrum taken on October 1 was calibrated using the z-band photometry of September 30, while the zJ spectrum of October 20 was simply aligned with the HK segment, applying the same calibration factor. The resulting 0.95–2.35 μm spectra are shown in Fig. 3, while fluxes of the relevant features identified are listed in Table 3. Since both spectra were acquired during the declining phase, it is not surprising that they are similar to the LUCI2 spectrum obtained during the same phase of the 2015–2016 outburst (Giannini et al. 2017). The most prominent lines are the H I recombination lines of the Paschen and Brackett series, along with a couple of metallic lines of Fe I and O I that were not detected in 2016. The He I 1.08 μm line is also detected in both spectra and exhibits a weak PCyg-like absorption in the October 20 spectrum, which signals outflow activity. The H_2 2.12 μm emission is only detected when the source is close to quiescence (October 20); this also happened previously (Lorenzetti et al. 2015; Giannini et al. 2017). Likely, the line is not detected during outbursts owing to an unfavorable line-to-continuum ratio when the source is bright. The fact that the H_2 emission is substantially unrelated with the source brightness suggests that it comes from the diffuse cloud.

3. Results and discussion

3.1. Photometry

3.1.1. Increasing versus decreasing speed

As shown in Fig. 2, well-sampled monitoring of V1118 Ori was obtained for the last five outbursts, from the one occurred in 1997 to that of 2019. Therefore, V1118 Ori offers the unique possibility of comparing the speed of brightness variation (Δmag/Δt) calculated with the same method in subsequent events of the same EXor source. This speed can be easily obtained as the slope of the linear fit through the photometric points of the rising and declining phase (Fig. 1).

For the last outburst, we get $\Delta g/\Delta t = 0.018$ mag day^{-1} (rising) and 0.031 mag day^{-1} (declining). We estimated these values by considering as starting and ending points of the fit those from which the brightness starts (stops) to increase (decrease) monotonically. We note that this choice implies that the slope of 0.018 mag day^{-1} is the maximum speed value that can be fitted through the rising phase data.

The same method applied to the data of previous outbursts provides the $\Delta V/\Delta t$ reported in Table 4. Broadly speaking, the majority of both increasing and decreasing speed values range between 0.011 and 0.015 mag day^{-1}. Two significant exceptions are represented by the increasing speed of the 2005 outburst (0.035 mag day^{-1}) and the decreasing speed of the last event (0.031 mag day^{-1}). More importantly, the data in Table 4 show that while in 2005 the increase was faster (by more than a factor two) compared to the decrease, the reverse phenomenon occurred in the last outburst.

These differences provide indications that heating and cooling occur with different modalities in subsequent outburst events. We speculate that a role might be played by the temperature reached at the outburst peak, the quantity of gas inside the

[3] http://www.iasf-milano.inaf.it/Research/lbt_rg.html

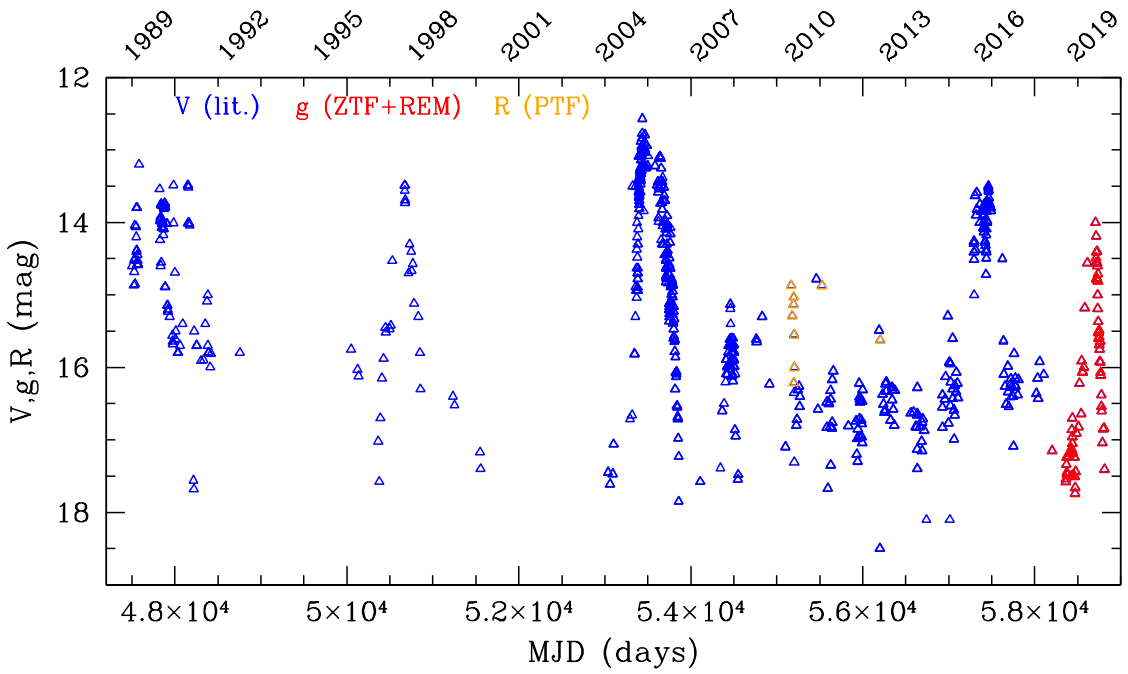

Fig. 2. Thirty-year period of the optical light curve of V1118 Ori. *V*-band data taken from Giannini et al. (2017) and references therein (mainly Audard et al. 2010). *R*-band photometric points retrieved from the Palomar Transient Factory survey are depicted in orange. The ZTF+REM *g*-band data of the 2019 outburst are shown in red.

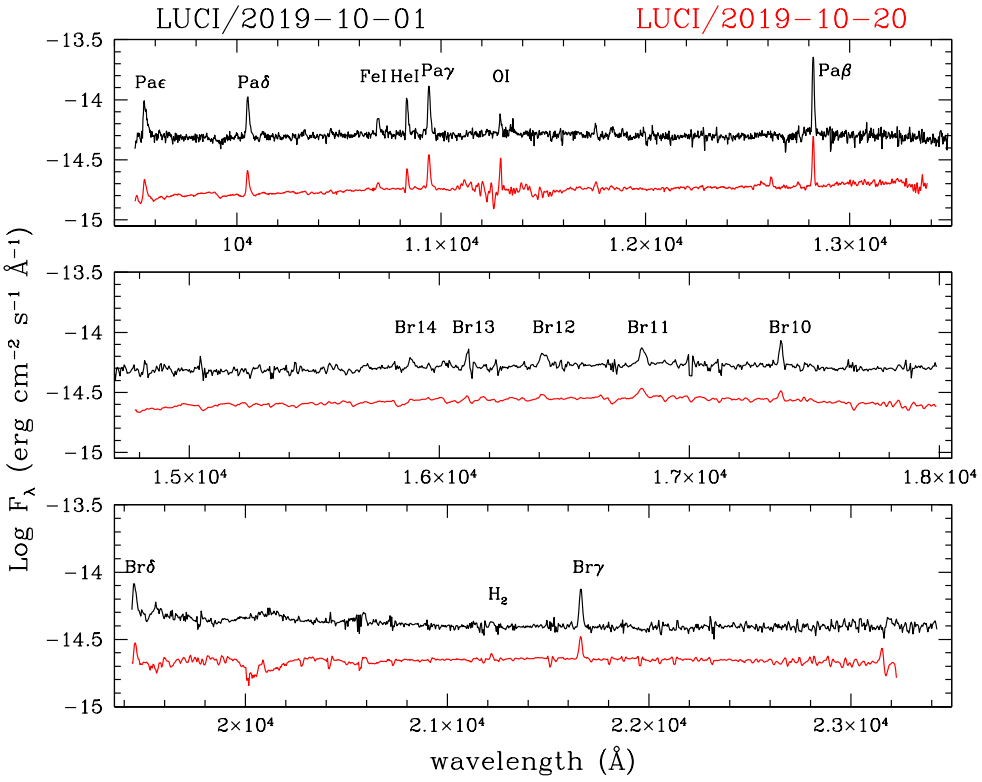

Fig. 3. Near-IR spectra taken on October 1 (black) and October 20 (red). The main emission lines are labeled.

accretion columns, and the fraction of the stellar surface involved in the accretion shocks. Indeed, very different scenarios for the outburst dynamics are predicted by theoretical models, from two ordered funnel streams forming two hot spots on the stellar surface (e.g., Romanova et al. 2004) to multiple unstable "tongues" of matter that form chaotic spots with irregular shapes and positions (e.g., Romanova et al. 2008).

3.1.2. Possible outburst periodicity

In general, the intermittence of the EXor's outbursts does not show any clear periodicity and, considering Fig. 2, V1118 Ori seems to obey the same trend. However, to have a more quantitative confirmation, we performed the Lomb–Scargle analysis for all available photometries (*V* and *g* bands) collected in the

Table 3. Line fluxes.

Line	λ_{vac} (Å)	01 Oct. 2019 $F \pm \Delta F$ (10^{-14} erg s^{-1} cm^{-2})	20 Oct. 2019 $F \pm \Delta F$ (10^{-14} erg s^{-1} cm^{-2})
Paϵ	9549	9.7 ± 0.6	2.19 ± 0.05
Paδ	10052	10.1 ± 0.4	2.19 ± 0.05
Fe I	10691	3.4 ± 0.3	0.49 ± 0.05
He I	10832	6.3 ± 0.3	(-0.1) [a] 1.00 ± 0.03
Paγ	10941	11.7 ± 0.3	3.49 ± 0.02
O I	11290	2.5 ± 0.3	0.41 ± 0.03
Paβ	12821	19.7 ± 0.5	3.84 ± 0.03
Br14	15885	2.0 ± 0.5	–
Br13	16114	2.5 ± 0.8	–
Br12	16413	4.5 ± 1.0	1.0 ± 0.1
Br11	16811	5.5 ± 0.4	1.8 ± 0.2
Br10	17366	5.5 ± 0.4	2.0 ± 0.1
Brδ	19451	7.7 ± 0.6	1.7 ± 0.2
H_2	21218	<0.5 [b]	0.3 ± 0.1
Brγ	21661	6.7 ± 0.2	1.9 ± 0.1

Notes. [a]P Cyg-like absorption. [b]3-σ upper limit.

Table 4. Brightness variation speed observed during the last four outbursts of V1118 Ori.

Outburst (year)	R (rise) (mag day^{-1})	D (decline) (mag day^{-1})	R/D
1997 [a]	0.011	0.013	0.85
2005 [a]	0.035	0.015	2.33
2015 [a]	0.015	0.015	1.00
2019 [b]	0.018	0.031	0.58

Notes. [a]V-band data. [b]g-band data.

last 30 years. The resulting periodogram is characterized by several peaks with little statistical significance mainly due to a very noisy quiescence level and unevenly sampled data. In any case, the presence of multiple peaks does not favor a periodical behavior of the outburst events.

3.1.3. Two-colors plot

The two-color diagram $[g - r]$ versus $[r - i]$ derived from REM data (blue dots) is presented in Fig. 4. For comparative purposes, we also show the colors of the period 2005–2016, taken from Audard et al. (2010) and Giannini et al. (2017). These were obtained from the original Johnson-Cousins photometric points VR_cI_c transformed into Sloan magnitudes[4]. Different symbols and colors indicate different outburst episodes ($V < 16.5$) and subsequent post-outburst periods ($V \geq 16.5$). Colors of the low-mass young stellar population in Praesepe and Coma Berenices (400–600 Myr) from spectral types F8 to M3 (Kraus & Hillenbrand 2007) are also depicted as black triangles. The direction of the extinction vector is represented, adopting the Cardelli et al. (1989) extinction law.

The main difference among the three outbursts illustrated in Fig. 4 lies in the gradual blueing of the color $[g - r]$, which on average is (in mag) 1.29 in 2005, 1.00 in 2015, and 0.73 in 2019.

[4] http://www.sdss3.org/dr8/algorithms/sdssUBVRITransform.php

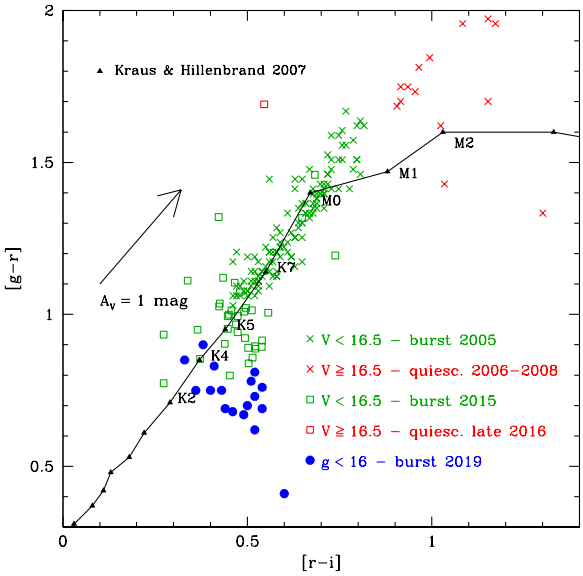

Fig. 4. Diagram of $[g - r]$ vs. $[r - i]$. The blue dots represent the points of the 2019 outburst. The green symbols indicate the points of the 2005 and 2015 outbursts ($V < 16.5$, crosses and open squares), while red symbols indicate the colors of the subsequent quiescence phases ($V \geq 16.5$). Transformation equations between Johnson–Cousins and Sloan photometric systems have been applied. The continuous line indicates the locus of 400−600 Myr young stars (Kraus & Hillenbrand 2007). The black arrow denotes the extinction vector for $A_V = 1$ mag, adopting the Cardelli et al. (1989) extinction law.

We note that this behavior cannot be attributed to a continuous decrease of the visual extinction since, as we show in Sect. 3.2.2, the A_V measured during the three outbursts was roughly the same ($A_V \sim 1.5$ mag). Therefore, we interpret the steadily decreasing $[g - r]$ value over the past 15 years with a gradual increase in the temperature of the photosphere during subsequent outbursts. Vice versa, the color $[r - i]$ remains almost unchanged during the three outbursts; the average $[r - i]$ values are 0.62, 0.47, and 0.47 mag in 2005, 2015, and 2019, respectively. Therefore, the variations of $[r - i]$ are likely to be driven by mechanisms not closely related to the outburst episodes.

3.2. Near-IR spectroscopy

3.2.1. Equivalent width versus continua

As a benefit of dealing with outbursts of the same source, we can examine in detail the simultaneous variability of the continuum and line emission, removing any significant contamination that can arise when considering multiple sources (for example, having different disk inclinations). In particular, we consider the line emission that likely originates in the accretion columns close to the stellar surface (prominent H I recombination; Muzerolle et al. 1998; Alcalá et al. 2014, 2017) in phases characterized by a different level of activity. As a premise, a correlation between Hα and Hβ fluxes and R- and B-band continua was highlighted in a sample of EXors (Lorenzetti et al. 2015 and references therein). This supports the idea that accretion-driven mechanisms explain both line and continuum variability.

In this work, we compare the equivalent width (EW) of H I recombination lines with the underlying continuum. Having examined all the spectra of V1118 Ori that we collected so far (Lorenzetti et al. 2006, 2015; Giannini et al. 2016, 2017), we show in Fig. 5 the EW variations of both the optical (Hβ

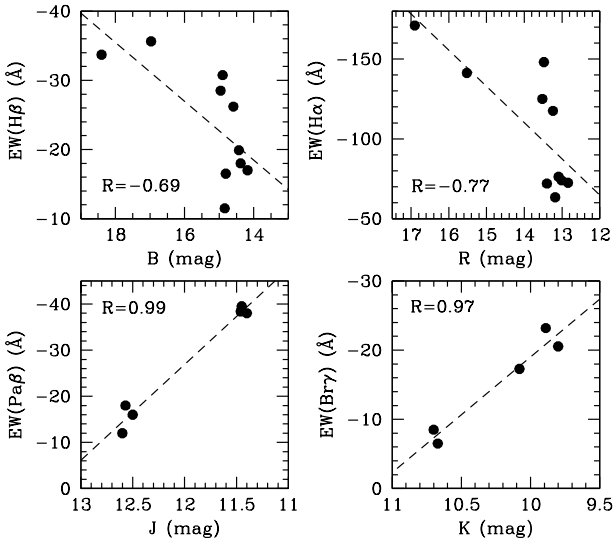

Fig. 5. Equivalent width of optical (*upper panels*) and near-IR (*lower panels*) H I recombination lines as a function of the underlying continuum (in magnitudes). In each panel, the linear fit through the data is shown with a dashed line, and the correspondent regression coefficient is indicated.

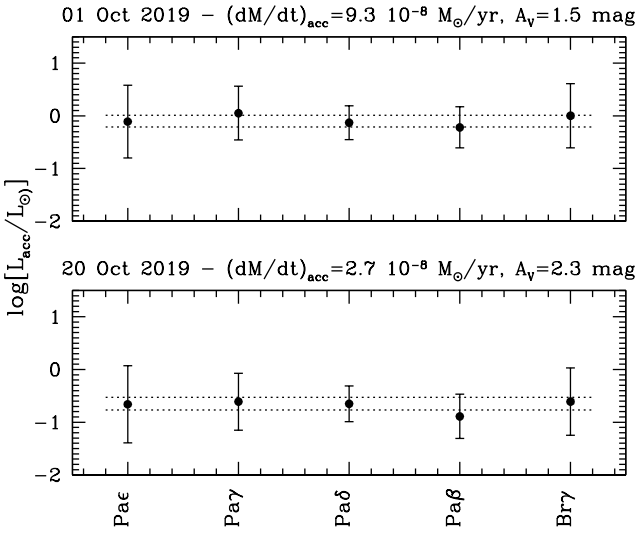

Fig. 6. Accretion luminosity derived by applying the Alcalá et al. (2017) empirical relationships between L_{acc} and the luminosity of the indicated H I lines. The value L_{acc} is derived by iteratively adjusting the A_V value to minimize the spread among the individual $L_{acc}(i)$ derived by each line i. The error bars in the data points take into account the flux errors of Table 3 along with the uncertainties in the Alcalá et al. relationships. The dashed lines in each panel delimit the statistical error on L_{acc}. The date of the observation, the $\dot{M}_{acc}$ derived from L_{acc} applying the Gullbring et al. (1998) formula, and the fitted A_V are reported at the top of each panel.

and Hα) and near-IR (Paβ and Brγ) lines as a function of the magnitude of the continuum, taken almost simultaneously. Confirming the results of previous studies (PV Cep, Cohen et al. 1981, V1647 Ori, Acosta-Pulido et al. 2007), there is an anti-correlation in the optical bands. More interestingly, there is a well-defined correlation between Paβ and Brγ fluxes and J and K magnitudes, which have regression coefficients of −0.99 and −0.97. This dual behavior of optical and near-IR lines is compatible with the different regions in which the lines and the continuum originate. The anti-correlation in the B and R bands indicates that the optical continuum varies more (or faster) than the Hβ and Hα line emission. This can be naturally explained considering that the continuum emission is related to the heating of the photosphere in the accretion shock, while H I lines arise in the cooling of the gas in the accretion columns. Therefore, the observed anti-correlation simply reflects different heating and cooling times. Conversely, J- and K-band continua originate in the innermost regions of the circumstellar disk. Although the near-IR photometric variations are the result of multiple processes (e.g., viscous heating), they primarily follow the heating (or cooling) of the disk in response to the increase (or decline) in the temperature of the photosphere (Lorenzetti et al. 2007). As a consequence, J- and K-band continua are subject to a lower variation than H I lines because the disk is more distant from the star than the accretion columns. Anyhow, both the correlation and anti-correlation exclude an extinction-driven origin of the variability, since in that case EW values should be constant for any fluctuation of the continuum.

3.2.2. Mass accretion rate and extinction variability

The mass accretion rate on the dates of the spectroscopic observations is derived by the empirical relationships between accretion luminosity (L_{acc}) and luminosity of lines in the accretion columns (L_{line}), determined in a sample of T Tauri stars in Lupus by Alcalá et al. (2017). Among the lines observed in the 2019 spectra, those for which such relationships are available are the Paschen lines from Paϵ to Paβ plus the Brγ line. First, each line flux was converted into L_{line} by adopting a distance to V1118 Ori of 400 pc (Muench et al. 2008). Then, L_{acc} is estimated together with the visual extinction A_V with a recursive fitting method (for a detailed explanation see Giannini et al. 2018). The mass accretion rate, $\dot{M}_{acc}$, derives from L_{acc} through the formula of Gullbring et al. (1998), taking $M_* = 0.4\,M_\odot$ $R_* = 1.29\,R_\odot$ (Hillenbrand 1997; Stassun et al. 1999) and a typical disk inner radius $R_{in} = 5\,R_\odot$.

The fit results are shown in Fig. 6 and listed in Table 5, where they are compared with the determinations of other outbursts and quiescence periods we derived by applying the same method. For the 2019 outburst, we measure a maximum $\dot{M}_{acc}$ of $\sim 10^{-7}\,M_\odot\,yr^{-1}$, which is similar to the value reached in the outburst of 2015 and a factor of ten less than that of 2005. In Table 5 we also give the fitted values of the visual extinction. Interestingly, except for the last measurement in October 2019, the A_V variation follows the evolution of brightness. The maximum A_V

Table 5. Extinction, accretion luminosity, and mass accretion rate between 2005 and 2019.

Date	Status	A_V (mag)	L_{acc} ($L_\odot$)	$\dot{M}_{acc}$ ($10^{-7}\,M_\odot\,yr^{-1}$)
Late 2005 [a]	Outburst peak	1.4	–	∼10
11 Sep. 2005	Declining	0.7	1.3	1.70
25 Mar. 2014	Quiescence	2.5	0.02	0.025
12 Jan. 2016	Outburst peak	1.5	1.1	1.25
31 Jan. 2016	Outburst peak	1.5	0.85	1.09
04 Dec. 2016	Quiescence	0.5	0.025	0.035
01 Oct. 2019	Outburst peak	1.5	0.72	0.93
20 Oct. 2019	Declining	2.3	0.21	0.27

Notes. [a]Taken from Audard et al. (2005).

of 2.5 mag is found in 2014 at the end of a long quiescence period that lasted about ten years, while $A_V \sim 1.5$ mag is measured at the peak of all three outbursts. The minimum A_V (<1 mag) is reached during the decline phase both in 2005 and 2016. This A_V variability might be explained in the scenario in which the onset of an outburst occurs when the material accumulated in the inner disk reaches a threshold value that corresponds to the maximum of A_V. The outburst continues until the reservoir of material is over (namely the minimum of A_V) and then the material starts to accumulate again with a consequent increase of A_V. Support for this scenario might be found in the case in which a significant area of the V1118 Ori (circumbinary) disk was intercepted by the line of sight. Unfortunately, the inclination of the V1118 Ori disk remains unknown even after dedicated Atacama Large Millimeter/submillimeter Array observations (Cieza et al. 2018).

4. Final remarks

We presented the optical photometry and near-IR spectroscopy of the last outburst of the classical EXor V1118 Ori, which occurred in the period January−October 2019. This one is the fifth well-sampled outburst, since 1989, characterized by a variation in brightness greater than three g-band magnitudes. Comparing the properties of the last event with those of the previous events, we can summarize the similarities and salient differences as follows:

– The outburst amplitude of the last event is similar to that of 1989, 1998, and 2015. The 2005 outburst remains the brightest. The duration is roughly the same (less than one year) for all.

– The historical light curve shows no evident periodicity, thus favoring accretion-driven rather than extinction-driven mechanisms as triggers of the outburst.

– The latest outburst showed different increase and decrease speeds of 0.018 and 0.031 mag day^{-1}, as opposed to the 2005 outburst, when the increase was faster (by more than a factor two) compared to the decrease. This hints at different modalities that both regulate heating and cooling and vary from event to event.

– The last three outbursts showed a gradually blueing $[g-r]$ color that we interpret with a gradual increase in the temperature of the photosphere. No significant variation is found in the $[r-i]$ color.

– The low-resolution near-IR spectrum, taken near the peak of brightness, is similar to that of 2015 (in 2005 no near-IR spectra were taken). Main emission lines are the H I Paschen and Brackett lines. As observed in 2015, He I 1.08 μm has a P Cyg-like profile that signals outflow activity. Faint metallic lines emission is present.

– The EW of the H I optical lines (Hα and Hβ) are anti-correlated with the R- and B-band continua, while the EW of the near-IR lines (Paβ, Brγ) are closely correlated with J- and K-band continua. This indicates that all the lines (both optical and near-IR) originate at the same distance from the star (i.e., in the accretion columns), intermediate between the stellar surface and the inner disk, where most of the optical and infrared continua are emitted, respectively.

– The evolution of the mass accretion rate of the last outburst is similar to that of 2015, with a peak of $\dot{M}_{\rm acc}$ around $10^{-7}\,M_\odot\,{\rm yr}^{-1}$ and a decrease down to $\sim 3\times10^{-8}\,M_\odot\,{\rm yr}^{-1}$ in about a month. The evolution of the extinction during the last three outbursts was also probed and tentatively interpreted in the context of the variability of the source.

In conclusion, our analysis has demonstrated that the comparison of different outbursts of the same source is a nontrivial exercise, but rather it allows to put useful observational constraints for models of EXor phenomena.

Acknowledgements. The authors sincerely thank Mario Lattanzi for providing information on the *Gaia* observations of V1118 Ori and Gianluca Li Causi for his suggestions and constructive discussions. We aknowledge the italian LBT and REM teams for their support for both observations and data reduction. This work is based on observations obtained with with different instruments: [1] the Samuel Oschin 48-inch Telescope at the Palomar Observatory as part of the Zwicky Transient Facility project; [2] the Large Binocular Telescope (LBT). The LBT is an international collaboration among institutions in the United States, Italy and Germany. LBT Corporation partners are: The University of Arizona on behalf of the Arizona university system; Istituto Nazionale di Astrofisica, Italy; LBT Beteiligungsgesellschaft, Germany, representing the Max-Planck Society, the Astrophysical Institute Potsdam, and Heidelberg University; The Ohio State University, and The Research Corporation, on behalf of The University of Notre Dame, University of Minnesota and University of Virginia; [3] the Rapid Eye Mount (REM) Telescope, La Silla, Chile.

References

Acosta-Pulido, J. A., Kun, M., Ábrahám, P., et al. 2007, AJ, 133, 2020
Alcalá, J. M., Natta, A., Manara, C. F., et al. 2014, A&A, 561, 2
Alcalá, J. M., Manara, C. F., Natta, A., et al. 2017, A&A, 600, A20
Audard, M., Güdel, M., Skinner, S. L., et al. 2005, ApJ, 635, L81
Audard, M., Stringfellow, G. S., Güdel, M., et al. 2010, A&A, 511, 63
Audard, M., Ábrahám, P., Dunham, M. M., et al. 2014, Protostars Planets VI (Tucson: University of Arizona Press), 387
Bell, K. R., & Lin, D. N. C. 1994, ApJ, 427, 987
Bonnell, I., & Bastien, P. 1992, ApJ, 401, L31
Cardelli, J. A., Clayton, G. C., & Mathis, J. S. 1989, ApJ, 345, 245
Cieza, L. A., Ruíz-Rodríguez, D., Perez, S., et al. 2018, MNRAS, 474, 4347
Cohen, M., Kuhi, L. V., Harlan, E. A., et al. 1981, ApJ, 245, 920
D'Angelo, C. R., & Spruit, H. C. 2010, MNRAS, 406, 1208
Giannini, T., Lorenzetti, D., Antoniucci, S., et al. 2016, ApJ, 819, L5
Giannini, T., Antoniucci, S., Lorenzetti, D., et al. 2017, ApJ, 839, 112
Giannini, T., Munari, U., Antoniucci, S., et al. 2018, A&A, 611, A54
Giunta, A., Giannini, T., Antoniucci, S., et al. 2019a, ATel, 12774, 1
Giunta, A., Giannini, T., Vitali, F., et al. 2019b, ATel, 13298, 1
Gullbring, E., Hartmann, L., Briceño, C., & Calvet, N. 1998, ApJ, 492, 323
Hartmann, L., & Kenyon, S. J. 1985, ApJ, 299, 462
Herbig, G. H. 1989, European Southern Observatory Conference and Workshop Proceedings, 233
Herbig, G. H. 2008, AJ, 135, 637
Hillenbrand, L. A. 1997, AJ, 113, 1733
Kóspál, Á., Ábrahám, P., Goto, M., et al. 2011, ApJ, 736, 72
Kraus, A. L., & Hillenbrand, L. A. 2007, AJ, 134, 2340
Lodato, G., & Clarke, C. J. 2004, MNRAS, 353, 841
Lorenzetti, D., Giannini, T., Calzoletti, L., et al. 2006, A&A, 453, 579
Lorenzetti, D., Giannini, T., Larionov, V. M., et al. 2007, ApJ, 665, 1182
Lorenzetti, D., Larionov, V. M., Giannini, T., et al. 2009, ApJ, 693, 1056
Lorenzetti, D., Antoniucci, S., Giannini, T., et al. 2015, ApJ, 802, 24
Muench, A., Getman, K., Hillenbrand, L., et al. 2008, Handbook of Star Forming Regions, I, 483
Muzerolle, J., Hartmann, L., & Calvet, N. 1998, AJ, 116, 2965
Romanova, M. M., Ustyugova, G. V., Koldoba, A. V., et al. 2004, ApJ, 610, 920
Romanova, M. M., Kulkarni, A. K., & Lovelace, R. V. E. 2008, ApJ, 673, L171
Sicilia-Aguilar, A., Kóspál, Á., Setiawan, J., et al. 2012, A&A, 544, A93
Shu, F. H., Najita, J., Ruden, S. P., & Lizano, S. 1994, ApJ, 429, 797
Stassun, K. G., Mathieu, R. D., Mazeh, T., & Vrba, F. J. 1999, AJ, 117, 2941
Vorobyov, E. I., & Basu, S. 2015, ApJ, 805, 115